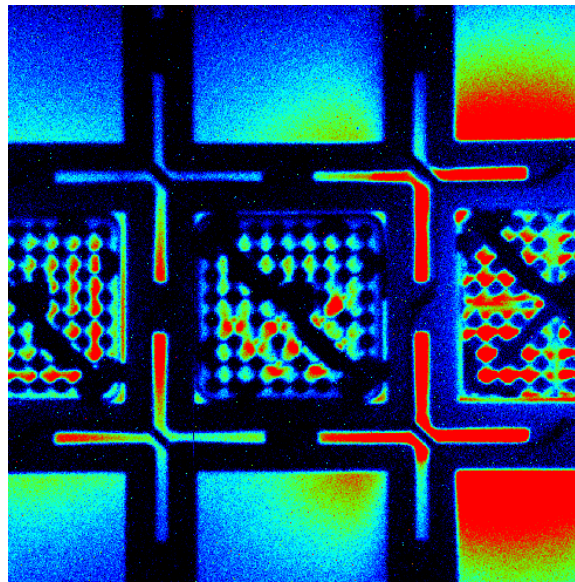




CSSP Report 2004-01-01

SKI Report ISRN SKI-R-03/45

**CERENKOV CHARACTERISTICS OF BWR ASSEMBLIES
USING A PROTOTYPE DCVD WITH
A BACK-ILLUMINATED CCD**



**Canadian and Swedish
Safeguards Support Programs**

**CERENKOV CHARACTERISTICS OF BWR ASSEMBLIES
USING A PROTOTYPE DCVD WITH A BACK-ILLUMINATED CCD**

Prepared for the Canadian Safeguards Support Program
and the Swedish Support Program

**J.D. Chen¹, A.F. Gerwing¹, R. Maxwell², M. Larsson³, K. Axell³,
L. Hildingsson³, B. Lindberg⁴ and E. Sundkvist⁵**

¹Channel Systems Inc., 402 Ara Mooradian Way, Pinawa, Manitoba R0E 1L0, Canada

²Canadian Nuclear Safety Commission, 280 Slater Street, Ottawa, Ontario K1P 5S9, Canada

³Swedish Nuclear Power Inspectorate, Klarabergsviadukten 90, SE-106 58 Stockholm, Sweden

⁴LENS-TECH AB, Anbudsvägen 5, SE-931 64, Skellefteå, Sweden

⁵Teleca Design and Development, Telegrafgatan 8A, SE-169 84 Stockholm, Sweden

2003 November 12

**SKI: ISSN 1104-1374
CSSP TASK ID: DV011
IAEA TASK: JNT/A704**

CANADIAN NUCLEAR SAFETY COMMISSION AND
SWEDISH NUCLEAR POWER INSPECTORATE
DISCLAIMERS

The information provided in this publication is subject to the following provisions and any use of the information will constitute acceptance of these provisions.

The Canadian Nuclear Safety Commission and Swedish Nuclear Power Inspectorate are not responsible for the accuracy of the statements made nor the opinions expressed in this publication, and neither the Commission, Inspectorate nor the authors nor their contractors, subcontractors, consultants, and agents assume any liability with respect to any damage or loss of any kind incurred as a result of the use or disclosure of the information contained in this publication whether based on contract, tort including negligence, strict liability, or otherwise.

The Canadian Nuclear Safety Commission, Swedish Nuclear Power Inspectorate and its contractors, subcontractors, consultants, and agents make no warranties in connection with the information provided in this publication, and all merchantability, fitness for purpose, freedom from the infringement of patents or other privately held rights and including any warranties as to the accuracy, completeness, or usefulness, or the use or the results of the use of any of the information provided in this publication.

ABSTRACT

The Canadian and Swedish Safeguards Support Programs have developed a prototype Digital Cerenkov Viewing Device (DCVD) to verify spent fuel. Field measurements in Swedish nuclear power reactor fuel bays on BWR fuel and non-fuel assemblies resulted in new Cerenkov information that offers the possibility of computer-assisted verification of spent-fuel assemblies. A number of fuel assemblies with missing fuel rods were examined. The missing fuel rods are easily detected when not hidden under the lifting handle of the fuel assembly. Initial studies of off-angle viewing of these assemblies show promise for the detection of the missing fuel rods under the lifting handle. The quantitative nature of the charge-coupled device was examined. A number of procedures were developed to quantify parameters such as image intensity and alignment (collimation) of fuel and non-fuel assemblies. The quantitative studies on fuel assembly intensity as a function of cooling time showed excellent agreement with the theoretical calculations.

Document Revision History

Revision 0 2003 November 12

TABLE OF CONTENTS

1	INTRODUCTION.....	1
2	INSTRUMENTATION	1
3	EXPERIMENTAL RESULTS.....	1
3.1	CERENKOV CHARACTERISTICS OF BWR SPENT FUEL	2
3.2	INTENSITY MEASUREMENTS OF SPENT FUEL WITH DIFFERENT COOLING TIMES	5
3.3	NEAR-NEIGHBOUR EFFECT ON CERENKOV INTENSITY	6
3.4	INTENSITY MEASUREMENTS FROM THE FUELLING MACHINE AND WALKING BRIDGE..	7
3.5	CERENKOV CHARACTERISTICS OF BWR NON-FUEL ASSEMBLIES	8
3.5.1	BWR 8 x 8 skeleton non-fuel assembly, Ringhals Unit 1	8
3.5.2	BWR 8 x 8 skeleton, non-fuel assembly, Oskarshamn Unit 2.....	8
3.5.3	BWR high-density 8 x 8 non-fuel assembly, Oskarshamn Unit 2	9
3.5.4	BWR high-density SVEA-64 non-fuel assembly, Ringhals Unit 1	11
3.5.5	BWR SVEA-64 helium-filled-rods non-fuel assembly, Ringhals Unit 1	11
3.6	CERENKOV CHARACTERISTICS OF BWR FUEL ASSEMBLIES WITH MISSING RODS.....	12
3.7	SVEA-64 FUEL ASSEMBLY WITH 47 MISSING FUEL RODS	14
3.8	OFF-ANGLE VIEW OF NON-FUEL AND FUEL ASSEMBLIES	15
3.9	QUANTITATIVE CERENKOV CHARACTERISTICS—ALIGNMENT.....	16
3.10	CERENKOV LIGHT FALL-OFF FROM SHORT-COOLED SPENT FUEL.....	17
3.10.1	Correction for near-neighbour effects.....	17
3.10.2	Verification of burnup and cooling time.....	18
3.11	QUANTITATIVE NEAR-NEIGHBOUR CORRECTIONS	19
4	FUTURE WORK.....	21
5	CONCLUSION	21
6	ACKNOWLEDGEMENTS	21
7	REFERENCES.....	22

LIST OF FIGURES

Figure 1: The prototype DCVD mounted on a bridge.....2

Figure 2: Selection of brightest pixels for image intensity.....2

Figure 3: Normal camera images of BWR spent-fuel assemblies3

Figure 4: Mark IVe CVD images of BWR spent-fuel assemblies3

Figure 5: DCVD images of BWR spent-fuel assemblies.....3

Figure 6: False-colour DCVD images of BWR spent-fuel assemblies4

Figure 7: BWR spent fuel, with no fuel channel box4

*Figure 8: Fuel arrangement with burnups/cooling times of four fuel assemblies,
Oskarshamn Unit 2.....5*

Figure 9: Four fuel assemblies with similar burnups but different cooling times.....5

Figure 10: Histogram of pixel intensity—determination of intensity6

*Figure 11: Measured and calculated Cerenkov intensities (normalized) for four BWR
spent-fuel assemblies.....7*

Figure 12: The near-neighbour effect: fuel identification and intensities (counts).....7

Figure 13: BWR 8 x 8 skeleton non-fuel assembly, Ringhals Unit 19

Figure 14: BWR 8 x 8 skeleton non-fuel assembly, Oskarshamn Unit 2.....10

Figure 15: BWR high-density 8 x 8 non-fuel assembly, Oskarshamn Unit 210

Figure 16: BWR high density SVEA-64 non-fuel assembly, Ringhals Unit 1.....11

Figure 17: BWR helium SVEA-64 non-fuel assembly, Ringhals 112

Figure 18: BWR spent-fuel assembly with 10 missing rods13

Figure 19: BWR spent-fuel assembly with four missing fuel rods.....13

Figure 20: BWR spent-fuel assemblies with missing fuel rods.....14

Figure 21: BWR SVEA-64 non-fuel assembly, Oskarshamn Unit 214

Figure 22: SVEA-64 fuel assembly indicating the location of the 17 fuel rods.....15

Figure 23: BWR SVEA-64 assembly with 17 fuel rods.....15

Figure 24: Off-alignment images of SVEA-64 assembly with 17 fuel rods16

*Figure 25: Cerenkov characteristics of an Atrium 9 x 9 fuel assembly from non-aligned
positions.....16*

Figure 26: Alignment images for spent-fuel and non-fuel assemblies17

Figure 27: Selection of high intensity pixels in each quadrant18

Figure 28: Alignment characteristic as a function of off-alignment distance18

Figure 29: Fall-off of Cerenkov light from a spent-fuel assembly19

Figure 30: Intensity of Cerenkov light with distance from alignment20

Figure 31: Intensity values, measured and corrected for near-neighbour effects20

1 INTRODUCTION

In 1993, the Swedish and Canadian Safeguards Support Programs began a joint program to develop a high sensitivity Cerenkov viewing device (CVD). A commercial instrument based on a charge-coupled device (CCD) was purchased from AstroCam (Cambridge, UK) and subsequently tested at Swedish nuclear facilities. The results of these tests were documented in three reports^{1, 2, 3}. More recently, a new CCD camera system was purchased from Andor Technology (Belfast) and tested at the Central Interim Storage for Spent Fuel (CLAB) in Sweden on pressurized-water reactor (PWR) fuel and non-fuel, long-cooled boiling-water reactor (BWR) fuel, and Ågesta test reactor fuel assemblies⁴. This instrument is called the prototype digital Cerenkov viewing device (DCVD). It incorporates a Marconi back-thinned, UV-enhanced, 1024 × 1024 frame-transfer CCD with a UV quantum efficiency of 52%. The Andor camera was connected to a portable computer system based upon the PC/104-*plus* format. The Cerenkov images were viewed on a liquid crystal display (LCD). A railing bracket held the camera steady to obtain the Cerenkov images of the spent fuel. This instrument was successful in meeting the measurement objective of verification of a fuel assembly with a burnup of 10 000 MWd/t U and a cooling time of 40 years.

This report discusses studies carried out in Sweden at the Ringhals Nuclear Power Plant Unit 1 during the period January 14-24, 2002. Cerenkov characteristics of a variety of BWR spent-fuel and non-fuel assemblies using the prototype DCVD were examined. The prototype DCVD instrument studies on PWR fuel and non-fuel assemblies are published in a separate report⁵.

2 INSTRUMENTATION

The prototype DCVD was slightly modified as a result of the first field test of the instrument. New ergonomic handles were installed and the railing bracket was modified to hold the new handles on the camera. Details of the instrumentation can be found in the first field test report. The DCVD system mounted on the Oskarshamn walking bridge is shown in Figure 1.

3 EXPERIMENTAL RESULTS

This report will normally show visible light images of the fuel or non-fuel assembly taken with a digital camera, a Mark IVe CVD and a DCVD image. The visible light pictures were taken with a Nikon COOLPIX 990 digital camera with a 3X tele-extender. To obtain the CVD images, the Nikon camera was fitted to a Mark IVe CVD.

Because of the digital nature of the data, the brightness and contrast of images reproduced in this report can be and have been scaled to produce good images. It is difficult to directly compare image intensities in this report without examining the un-scaled, original data. For example, an assembly image that has only a few counts in each pixel (a long-cooled fuel or a short exposure time) can be scaled to look as bright as one that has many counts.

There are large regions of low counts (near black) in a DCVD image. These dark areas are fuel assembly parts such as fuel rods and the lifting handle. Therefore, quantitative intensity measurements obtained by averaging over an entire image are highly weighted

towards low counts. To obtain a more representative intensity for a fuel assembly, only the brightest pixels in an image are averaged. An explanation of the calculation procedure is given later in Section 3.2. Figure 2 shows an example of the selected bright pixels (red) used in an intensity calculation.

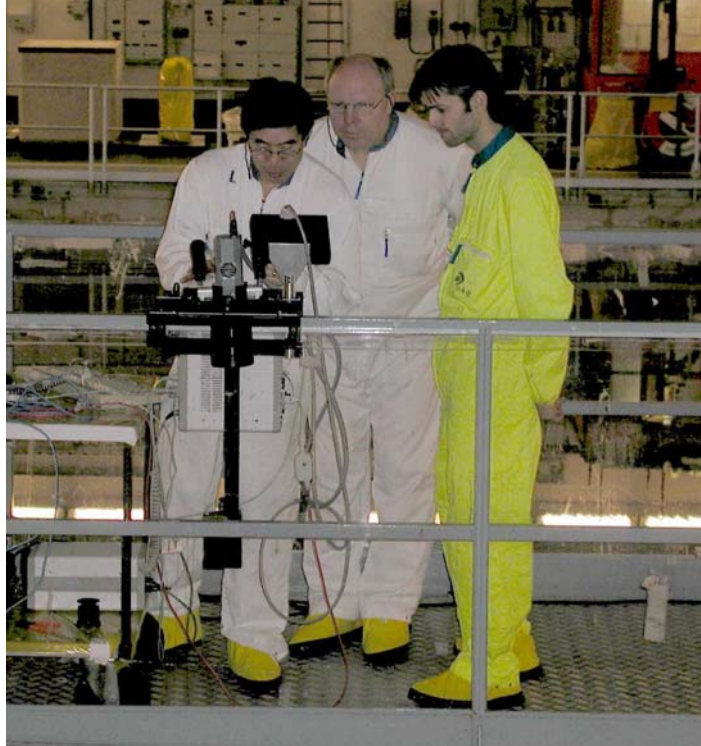


Figure 1: The prototype DCVD mounted on a bridge

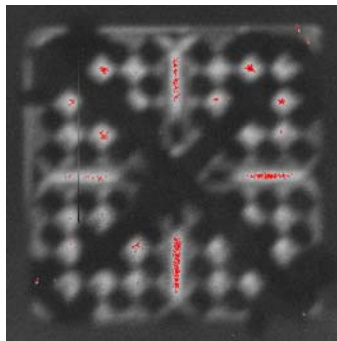
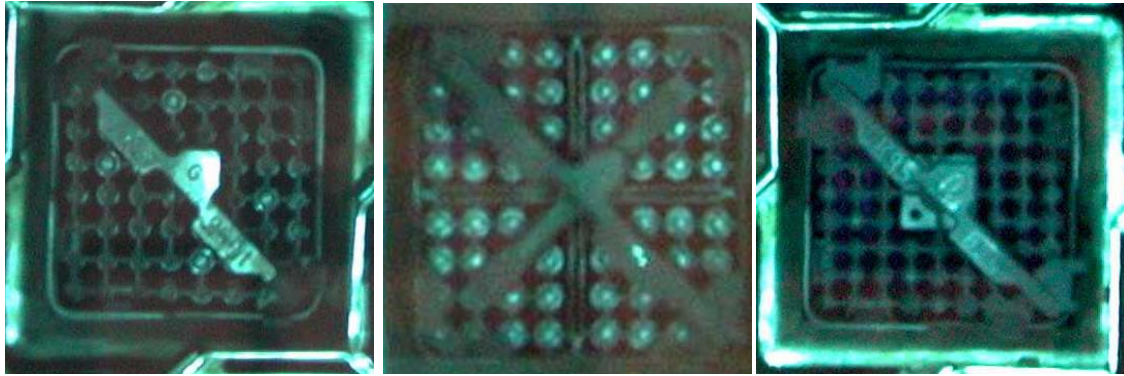


Figure 2: Selection of brightest pixels for image intensity

3.1 Cerenkov characteristics of BWR spent fuel

Three types of BWR fuel assemblies were examined. Camera pictures of Exxon ANF 8 x 8, ABB Atom SVEA-64 and a Siemens Atrium 9 x 9 are shown in Figure 3.

The CVD images for these fuel assemblies are shown in Figure 4 and the DCVD images are shown in Figure 5.

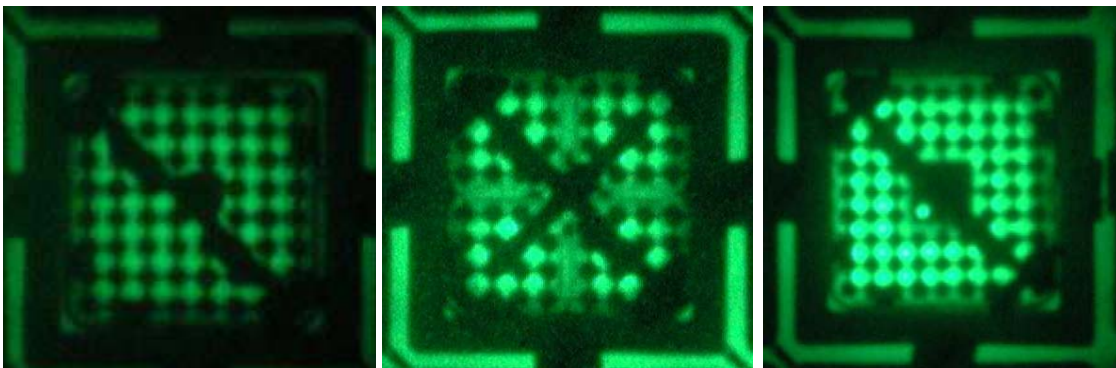


ANF 8 x 8

ABB Atom SVEA-64

Siemens Atrium 9 x 9

Figure 3: Normal camera images of BWR spent-fuel assemblies

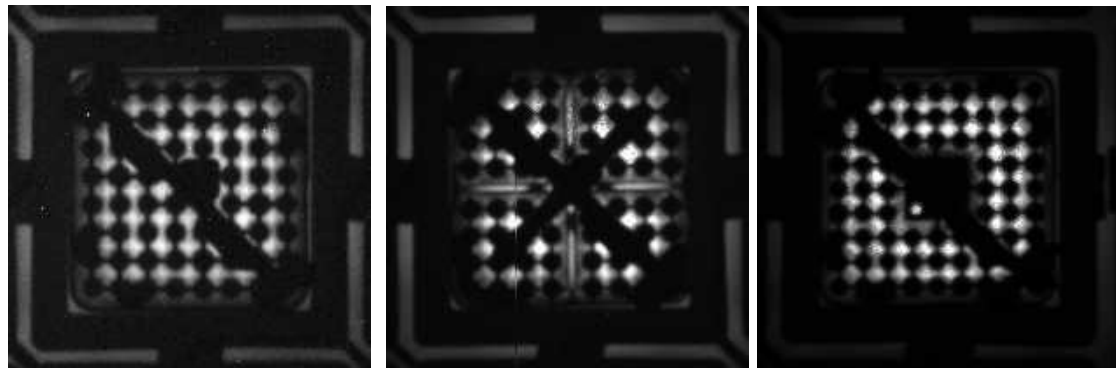


ANF 8 x 8

ABB Atom SVEA-64

Siemens Atrium 9 x 9

Figure 4: Mark IVe CVD images of BWR spent-fuel assemblies



ANF 8 x 8

ABB Atom SVEA-64

Siemens Atrium 9 x 9

Figure 5: DCVD images of BWR spent-fuel assemblies

The three types of fuel assemblies are very different in design. The ANF 8 x 8 is a 64-rod assembly that incorporates a water rod in the central region of the fuel assembly (under the handle) to increase the neutron flux in that region. The SVEA-64 and Atrium 9 x 9 are more advanced designs that further improve the burnup distribution and fuel performance. The SVEA-64 has four groups of 16 rods connected by an X-shaped mounting mechanism. There is a distinctive cross-shaped water channel (the “water cross”) that separates the four bundles. The Atrium 9 x 9 has a central zircaloy channel

replacing nine fuel rods. This zircaloy channel has four water inlets/outlets at each end. Only one water outlet can be seen when aligned above an assembly (Figure 3, Figure 4 and Figure 5).

The CVD images are similar to the DCVD images except that the digital images show higher resolution and certain features, such as the spacer grids, can be more easily detected. The spacer grids are indicated by the shading within the water spaces between the fuel pins (perhaps best seen in the DCVD image in Figure 19).

The false-colour images of these fuel assemblies, Figure 6, show a Cerenkov characteristic that is unique to spent fuel. The centres of the spent-fuel assemblies are brighter compared to the edges. This cannot be seen in the CVD images and is just discernible in the DCVD grey scale digital images in Figure 5. The colour bar on the right side indicates that blue is low intensity and red is high.

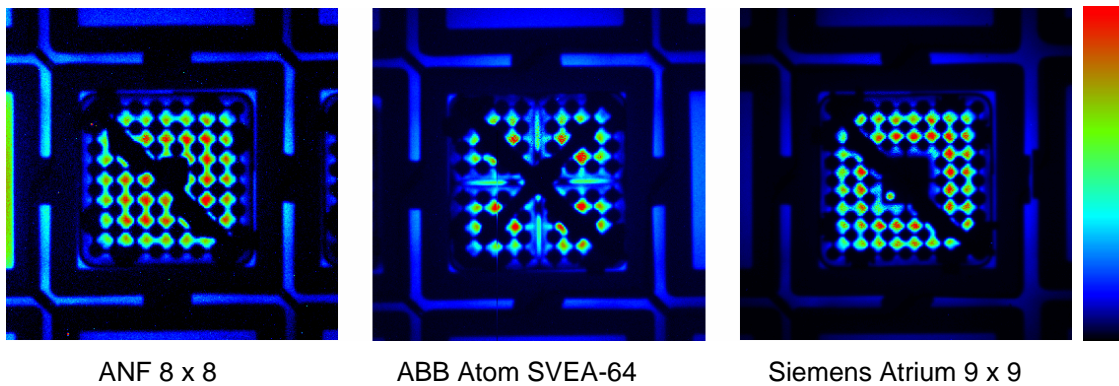


Figure 6: False-colour DCVD images of BWR spent-fuel assemblies

Figure 7 shows a normal camera, a Mark IVe CVD and a DCVD image of a long-cooled BWR fuel assembly (31 000 MWd/t U, 21-year-cooled). There is more room in the fuel storage site because of the absence of the fuel channel box (cf. a normal 8 x 8-fuel assembly with its channel box, Figure 5).

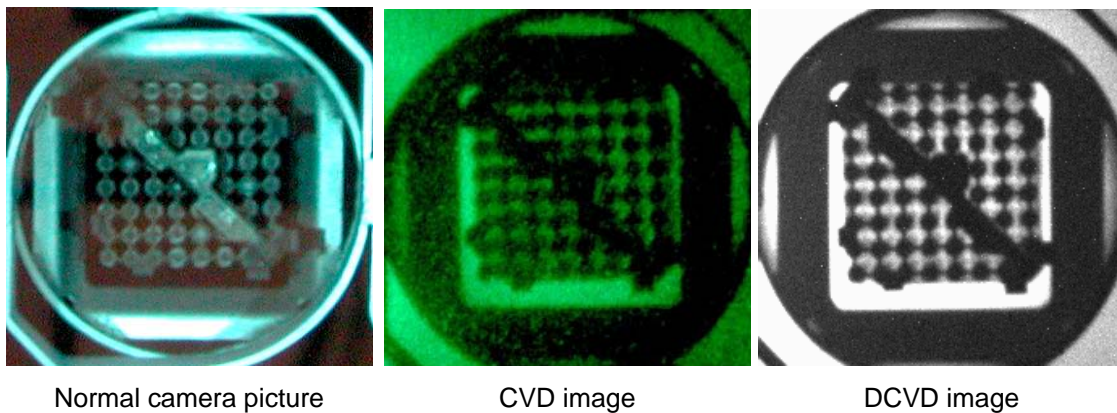


Figure 7: BWR spent fuel, with no fuel channel box

3.2 Intensity measurements of spent fuel with different cooling times

Four fuel assemblies were measured to determine their Cerenkov intensity as a function of cooling time. The burnups, cooling times and arrangement of the four fuel assemblies are shown in Figure 8. The first number is the burnup in megawatt days per kilogram uranium and the second number is the cooling time in years. The DCVD images for the fuels are shown in Figure 9.

39/2	38/4	38/6	39/5
------	------	------	------

Figure 8: Fuel arrangement with burnups/cooling times of four fuel assemblies, Oskarshamn Unit 2

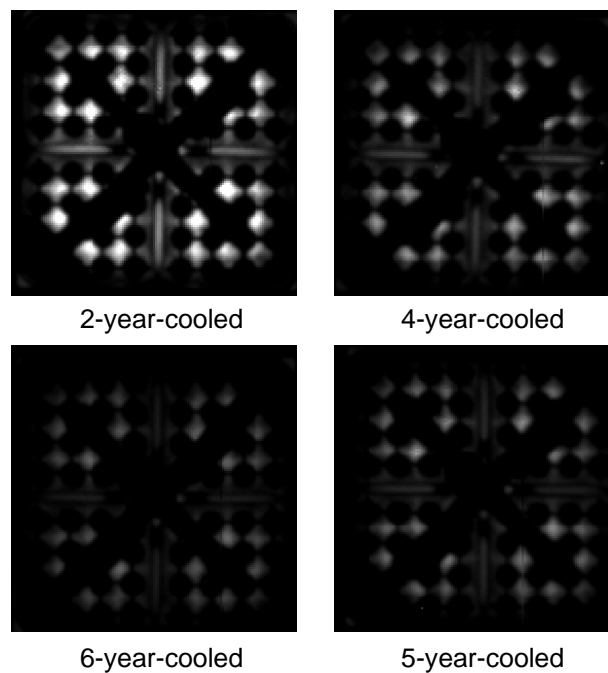


Figure 9: Four fuel assemblies with similar burnups but different cooling times

There are a number of methods to determine the Cerenkov light intensity of the individual fuel assemblies. One method is to subtract the background (DC offset, dark current, read noise) and calculate the average pixel intensity over the entire image. This method requires precise alignment over the fuel assembly to avoid biasing the results. An alternate method (similar to the technique used to scale images for live display on the DCVD system) selects only the brightest pixels in the fuel assembly. One percent of brightest pixels are ignored to reduce the effect of “hot” or “noisy” pixels. The intensity of the darkest pixel in the image is used as the background value and is subtracted from each of the pixels. Figure 10 shows a histogram of the pixels in the image for the 2-year-cooled fuel. Most of the image is dark, which is due to the structure of the fuel assembly (fuel rods, top plate and lifting handle). These dark pixels have very low counts and are not included in the calculated average for the assembly. There are a number of pixels at or near the maximum intensity. Typically, these pixels lie between 90% and 99% of the

maximum value. It is these pixels that are selected and their average value is calculated to represent the Cerenkov light intensity of the fuel assembly. The results for the four spent-fuel assemblies are given in Table 1.

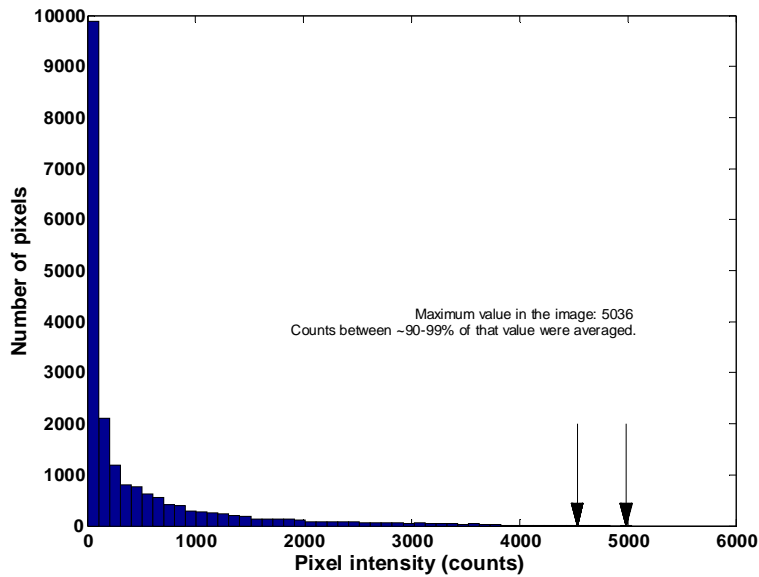


Figure 10: Histogram of pixel intensity—determination of intensity

The theoretically calculated photon fluxes of the four fuel assemblies, based upon earlier studies⁶, are given in the last column of Table 1. The data show the expected decrease in counts with cooling time. To compare the measured with the calculated results, the values were normalized to the brightest fuel and plotted in Figure 11. There is reasonably good agreement between the experimental and calculated values.

Table 1: Measured Cerenkov intensities of four fuel assemblies

Fuel ID	Burnup (MWd/t U)	Cooling time (years)	Intensity and precision (counts, 2σ)	Calculated photon flux (hv·cm ⁻² ·s ⁻¹)
19430	39 387	2	4685±230	2 105 602
18665	38 275	4	3054±144	1 276 202
18144	38 675	5	2358±20	983 178
15114	37 583	6	1719±84	841 599

3.3 Near-neighbour effect on Cerenkov intensity

An experiment was set up to assess the degree of cross talk between neighbouring fuel assemblies (the near-neighbour effect). This occurs when gamma rays from neighbouring fuel assemblies travel into the adjacent assembly and generate Cerenkov light in the water spaces. Figure 12 shows the fuel arrangement studied. Fuel assemblies 18655, 18699 and 18686 were measured.

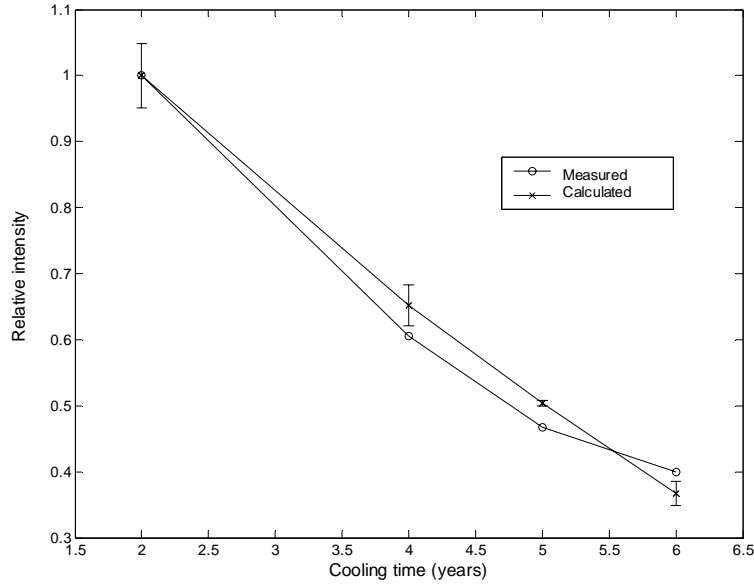


Figure 11: Measured and calculated Cerenkov intensities (normalized) for four BWR spent-fuel assemblies

Fuel assembly 18686 has four adjacent and one corner neighbour. Assembly 18699 has two adjacent and two corner neighbours and assembly 18655 has only one near neighbour. The measured intensities of these three assemblies are shown in Figure 12. The burnups and cooling times of the spent fuels are also indicated in the figure.

The data shows that relative to the top assembly, the next assembly has a 7% higher count rate and the third assembly, with the most near neighbours, has a 34% higher count rate. There is clearly a near-neighbour effect. When viewing these assemblies using the CVD, one cannot detect the intensity differences in these fuel assemblies.

	3512 18655 37/4	
	3744 18699 41/4	
SF 40/4	4693 18686 40/4	SF 41/1
	SF 38/4	SF 41/1

Figure 12: The near-neighbour effect: fuel identification and intensities (counts)

3.4 Intensity measurements from the fuelling machine and walking bridge

A fuel assembly was imaged from the walking bridge and the fuelling machine to compare the fuel’s intensity from the two heights. The observation distance (the top of

the rail to the top of the assembly) at O2 for the walking bridge and fuelling machine is 12.25 m and 12.89 m, respectively. The intensities measured at both positions are 4894 ± 336 and 4764 ± 278 , respectively. There is no statistical difference between these two values.

3.5 Cerenkov characteristics of BWR non-fuel assemblies

Three types of BWR non-fuel assemblies were examined at Oskarshamn Unit 2 and Ringhals Unit 1. They consisted of a skeleton assembly with no fuel rods (top and bottom nozzle and fuel channel box), a high-density assembly with lead- or steel-filled rods and an assembly with rods filled with helium gas. When isolated from other fuel assemblies, non-fuel assemblies are dark and do not emit any Cerenkov glow. However, they do appear to emit Cerenkov light when spent-fuel assemblies surround them. This is commonly referred to as the near-neighbour effect. These non-fuel assemblies were surrounded by relatively short-cooled fuel (1 to 5 years) to generate a Cerenkov glow within the non-fuel assembly. The Cerenkov glow is generated from the penetration of gamma rays from surrounding assemblies (near neighbours) into the water spaces in the non-fuel storage volume. The non-fuel assembly then appears to glow due to this near-neighbour effect.

3.5.1 BWR 8 x 8 skeleton non-fuel assembly, Ringhals Unit 1

Figure 13 shows a skeleton assembly from Ringhals Unit 1. The Mark IVe CVD image is very similar to the DCVD image. There are no rods present; the holes in the top plate where fuel rods are normally attached are clearly seen. The darker central square or shadow is unusual and appears to be a metal plate positioned somewhere in the middle of the assembly between the bottom and top plate. The false-colour image clearly shows the brighter regions in the image and provides better contrast in the square, shadow region under the lifting handle. The red colour (high intensity) also shows that the bottom part of the assembly is much brighter than the other sides and is probably caused by a 1-year-cooled near neighbour below the assembly. Its other near neighbours are 3-year-cooled spent fuels. It is obvious that this is not a spent-fuel assembly.

3.5.2 BWR 8 x 8 skeleton, non-fuel assembly, Oskarshamn Unit 2

Another skeleton assembly from Oskarshamn Unit 2 is shown in Figure 14. This assembly is obviously different than that shown in Figure 13: there is no shaded square (metal plate) in the centre of the image. This is a very bright non-fuel assembly since it contains no high-density gamma-absorbing materials. The CVD image shows low contrast and uniform glow distribution, which is evidence that the assembly is not generating its own Cerenkov glow. This assembly is easily identified as a non-fuel assembly.

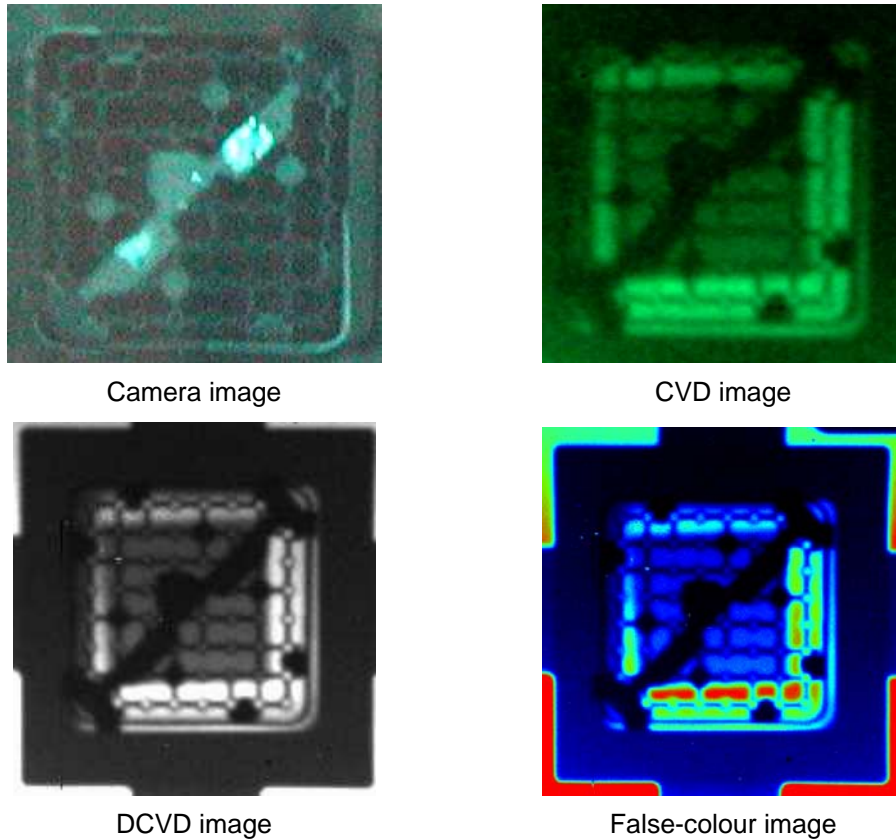
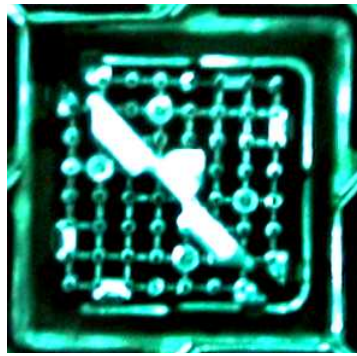


Figure 13: BWR 8 x 8 skeleton non-fuel assembly, Ringhals Unit 1

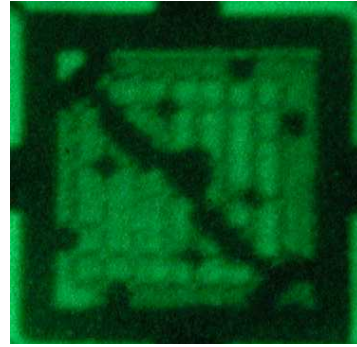
The DCVD image also shows a low contrast image but more details, such as the empty mounting holes in the top plate for the fuel rods. The false-colour image shows that the glow intensity has low contrast and is fairly uniform across the assembly, unlike spent fuel where the contrast is high and the light intensity at the centre of the assembly is higher than at the edges.

3.5.3 BWR high-density 8 x 8 non-fuel assembly, Oskarshamn Unit 2

The high density BWR 8 x 8 non-fuel assembly is constructed similarly to a fuel assembly, except that the fuel rods are filled with either lead or steel. This type of non-fuel assembly has the lowest glow intensity because of gamma ray absorption by the high-density rods. The Mark IVe CVD image (Figure 15) has low contrast and intensity. The DCVD image (Figure 15) also shows low intensity, but also that the centre of the assembly is darker than the edges. The gamma rays from the near neighbours are shielded by the high-density rods in the assembly resulting in a lower gamma ray flux in the centre. In spent fuel (cf. Figure 5), the centre of the assembly is brighter than the edges indicating that the assembly is generating its own Cerenkov light. The false-colour image clearly shows that the centre of the assembly is darker than the edges.



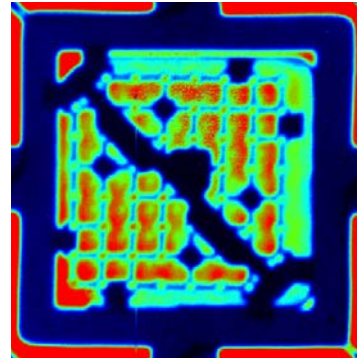
Camera image



CVD image

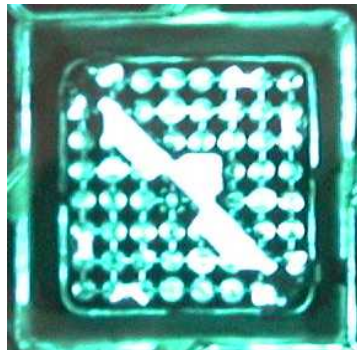


DCVD image

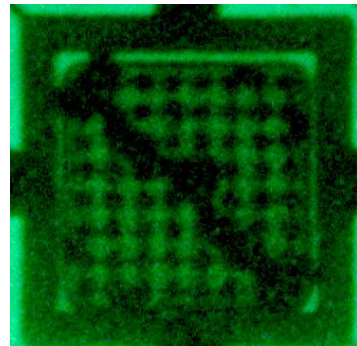


False-colour image

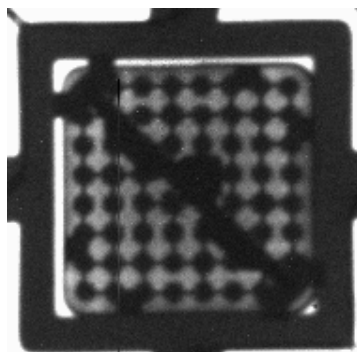
Figure 14: BWR 8 x 8 skeleton non-fuel assembly, Oskarshamn Unit 2



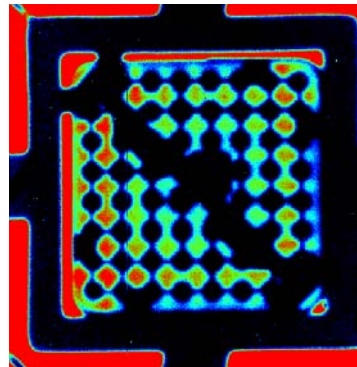
Camera image



CVD image



DCVD image



False-colour image

Figure 15: BWR high-density 8 x 8 non-fuel assembly, Oskarshamn Unit 2

3.5.4 BWR high-density SVEA-64 non-fuel assembly, Ringhals Unit 1

The SVEA-64 high-density non-fuel assembly, shown in Figure 16, is constructed similarly to a fuel assembly except that the rods are made of solid steel. The CVD image is very faint and the dark rods are difficult to resolve. The brightest feature is the relatively bright water-cross; it is higher in intensity than the light from between the fuel rods. This feature is opposite to the spent fuel characteristic (Figure 4) where the light from between the fuel rods is brighter than the light from the water cross. The higher-resolution digital image shows similar non-fuel Cerenkov characteristics. The top part of the water cross is brighter than the rest of the cross, which is probably due to a 1-year-cooled near neighbour adjacent to the top of the assembly; other near neighbours are 3-year-cooled spent fuel. In the false-colour image, these characteristics are easily seen. One can also see that the top part of the horizontal water cross is brighter than the bottom part of the water cross. This is probably due to the one-year-cooled diagonal near neighbour. The centre of the assembly appears to be darker than the edges in both the false-colour and DCVD image. This feature is characteristic of a non-fuel assembly.

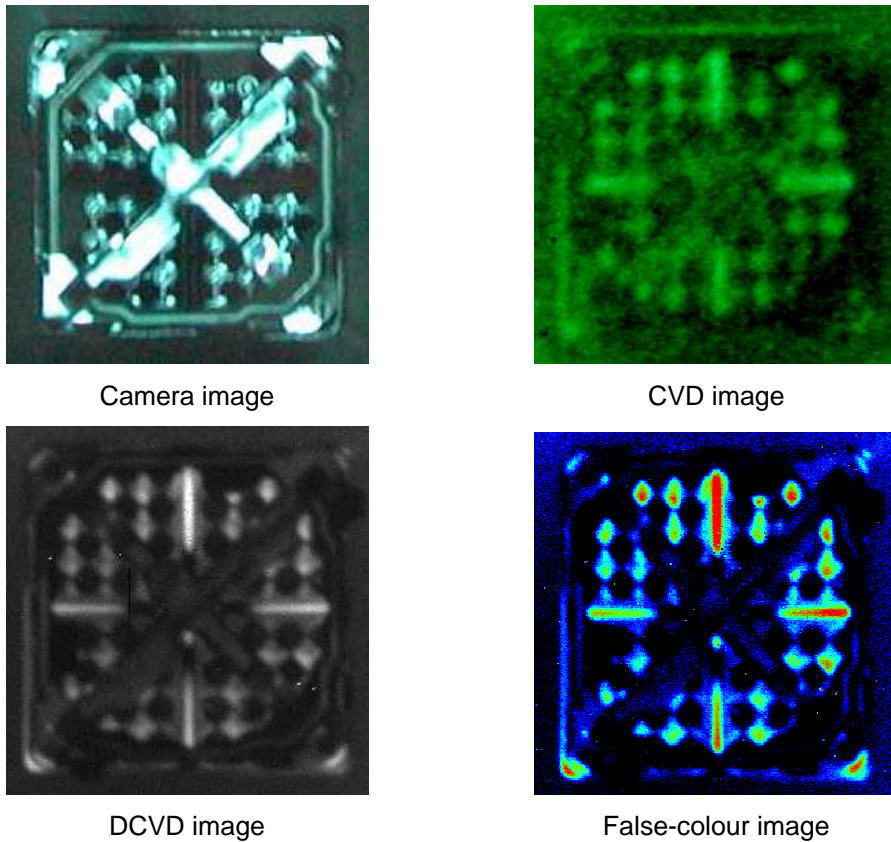


Figure 16: BWR high density SVEA-64 non-fuel assembly, Ringhals Unit 1

3.5.5 BWR SVEA-64 helium-filled-rods non-fuel assembly, Ringhals Unit 1

The SVEA non-fuel assembly, shown in Figure 17, is constructed similarly to a spent-fuel assembly except the rods are filled with helium. This non-fuel assembly was specifically manufactured by SKI to determine whether this type of non-fuel assembly could be detected using Cerenkov viewing devices. The non-fuel assembly has been used

at CVD training courses for IAEA inspectors. The camera image indicates that the metal surfaces have a shiny metallic finish. This non-fuel assembly has a relatively high Cerenkov glow intensity. This is attributed to the low-density rods and their shiny metallic surfaces, which reflect the Cerenkov glow generated by gamma rays emitted by adjacent spent-fuel assemblies. Furthermore, there is little attenuation by the low-density rods of the gamma flux from the near neighbours. From both the CVD and DCVD images, the water cross is brighter than the light from between the fuel rods. The DCVD image shows that the light intensity is fairly uniform across the assembly. These latter two characteristics are different from those of spent fuel, permitting the identification of this assembly as non-fuel.

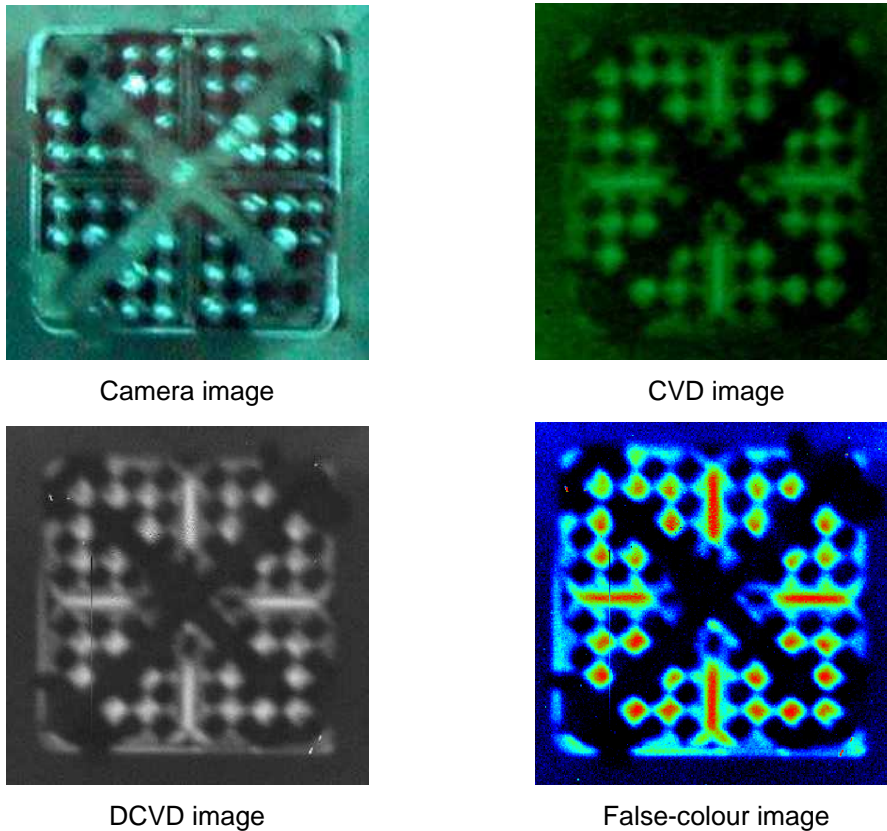


Figure 17: BWR helium SVEA-64 non-fuel assembly, Ringhals 1

3.6 Cerenkov characteristics of BWR fuel assemblies with missing rods

A BWR spent-fuel assembly with 10 missing rods is shown in Figure 18. This assembly has a long cooling time of 21 years and a low burnup of 9000 MWd/t U. The CVD image is very faint in the eyepiece and only seven missing rods can be identified. In the DCVD image, because of its higher sensitivity and higher resolution, it can be readily seen that there are nine missing fuel rods. In particular, the missing fuel rods close to the lifting handle can be identified. A tenth missing rod, located in the centre of the assembly, cannot be detected because it is under the handle.

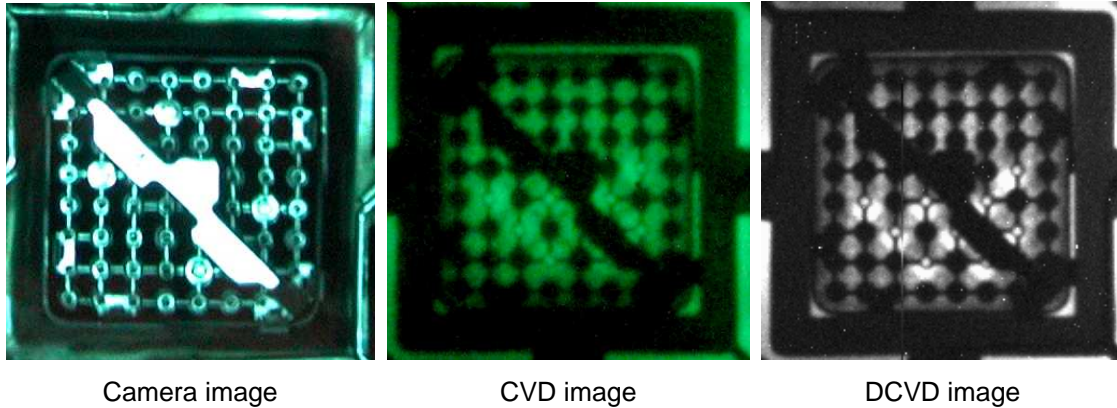


Figure 18: BWR spent-fuel assembly with 10 missing rods

Figure 19 shows an assembly with four missing fuel rods (24 000 MWd/t U burnup, 22-year-cooled). Three of the missing rods can be seen in both the CVD and DCVD images. The DCVD image also shows details, such as the well-defined empty fuel rod mounting holes in the top plate. The fourth missing fuel rod has been replaced with a zircaloy tube; it can be identified as the slightly larger pin adjacent to the lifting handle in the centre of the assembly (pin D4, in the numbering scheme shown in Figure 22). Perhaps the tube itself is larger or perhaps a larger bolt was used to fix the zircaloy tube to the top plate.

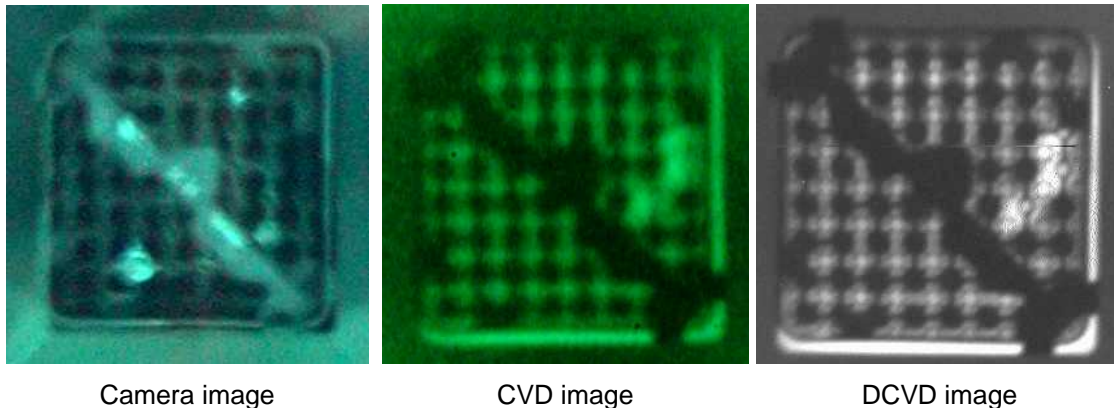
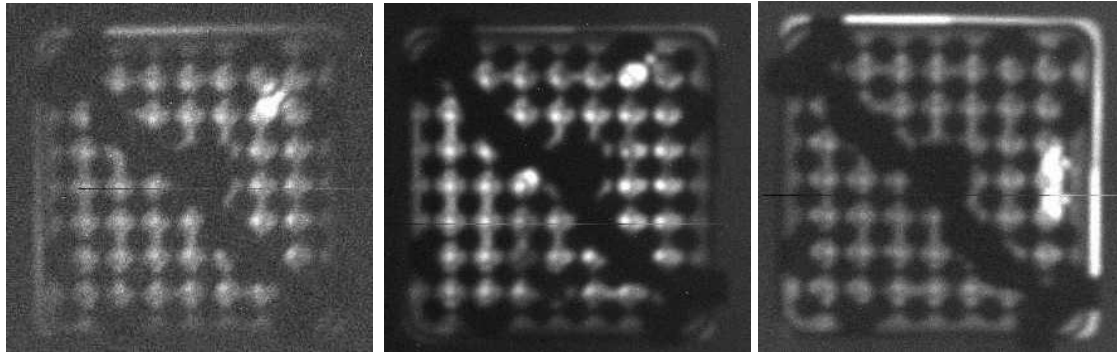


Figure 19: BWR spent-fuel assembly with four missing fuel rods

Figure 20 shows DCVD images of three fuel assemblies with missing fuel rods. These fuel assemblies have cooling times of 20 years or longer and approximate burnups of 22 000 MWd/t U. The assembly on the left has two missing fuel rods, one of which has been replaced with a zircaloy tube. The substituted pin is located near the lifting handle (pin D4, in the numbering scheme shown in Figure 22). The middle assembly has four missing fuel rods. An empty rod position can be seen near the top right hand corner of the assembly and the second missing fuel rod can be deduced because of a bright light close to the handle. A third missing fuel rod is under the handle and cannot be detected. The fourth missing fuel rod has been substituted with a zircaloy tube (pin position D4) near the centre of the assembly. The zircaloy tube cannot be detected in the DCVD image. The assembly shown in the right-hand image has three missing fuel rods. The two on the right hand side of the assembly are obvious. The missing fuel rod in the centre of the assembly

(rod position D4) has been replaced with a zircaloy tube. This tube is visible as a slightly larger pin.



One missing rod

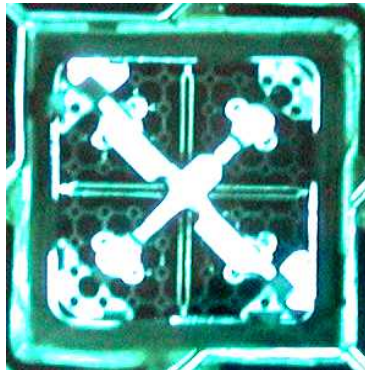
Two missing rods

Two missing rods

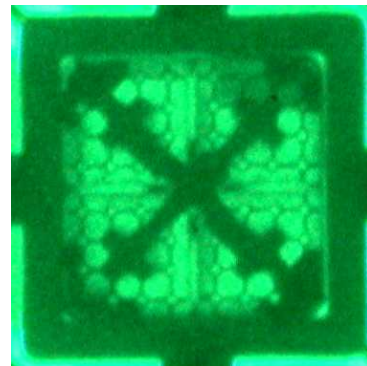
Figure 20: BWR spent-fuel assemblies with missing fuel rods

3.7 SVEA-64 fuel assembly with 47 missing fuel rods

The SVEA-64 assembly, shown in Figure 21, looks like a skeleton assembly with no fuel rods present. However, 17 rods are indeed present but are located under the cross mounting mechanism. Their positions are shown in Figure 22.



Camera image



CVD image

Figure 21: BWR SVEA-64 non-fuel assembly, Oskarshamn Unit 2

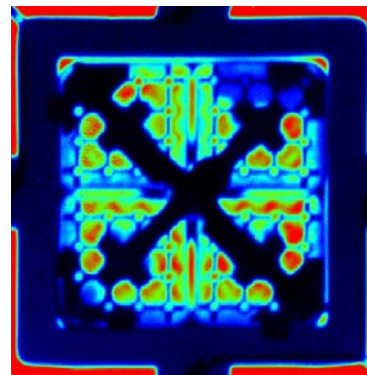
The principle components of the assembly (the fuel channel box, water cross, top and bottom plates and a mounting mechanism to hold the four quadrants together) can all be identified in the camera, CVD and DCVD images (Figure 23). No fuel rods can be detected. The DCVD Cerenkov image shows no evidence that fuel rods are present. The image shows low contrast while the light intensity in the water cross is similar in intensity to the light in the other areas of the assembly. The false-colour image shows considerably more detail. The areas at the ends of the mounting mechanism show areas of higher light intensity, a possible indication of the presence of fuel rods. These characteristics cannot be seen in the CVD image or the grey scale DCVD image. This is a good example illustrating the ability of false-colour display for the detection of missing fuel rods.

8								x
7		x	x			x		
6		x	x			x	x	
5								
4								
3		x	x			x	x	
2		x	x			x		
1	x							x
	A	B	C	D	E	F	G	H

Figure 22: SVEA-64 fuel assembly indicating the location of the 17 fuel rods



DCVD image



False-colour image

Figure 23: BWR SVEA-64 assembly with 17 fuel rods

3.8 Off-angle view of non-fuel and fuel assemblies

Cerenkov viewing device studies have always focused on the requirement for vertical alignment over the fuel to achieve maximum intensity, contrast and collimation. Perhaps additional characteristics are observable in an off-alignment image. Therefore, a number of DCVD measurements were made in steps of 2 cm up to 100 cm from vertical alignment. Measurements were taken in steps of 2 cm to, at times, up to 100 cm from the aligned position. The DCVD was tilted to maintain the assembly of interest in the centre of the field of view.

Figure 24 shows three images of the SVEA-64 assembly containing 17 fuel rods at different alignment positions.

The dark shadows of the fuel rods under the cross mounting brackets can be seen in the 12-cm off-alignment image and are obvious in the 25-cm off-alignment image (three are marked with arrows).

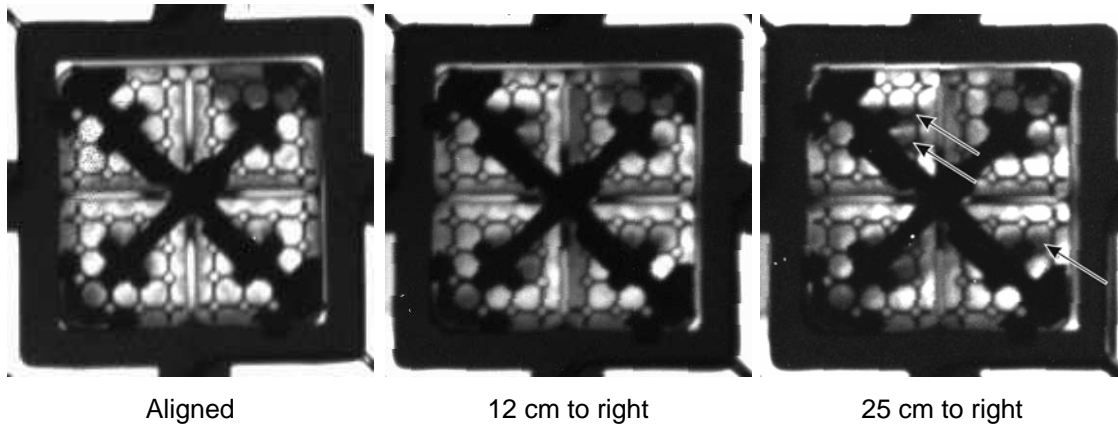


Figure 24: Off-alignment images of SVEA-64 assembly with 17 fuel rods

Figure 25 (left) shows a DCVD image of an aligned Atrium fuel assembly. The dark central water channel can be seen; one water outlet is visible. The second DCVD image taken from a position a row above and 25 cm to the right shows three of the four water outlets. The last DCVD image was taken at 37 cm to the right and shows all four water outlets of the central water channel. Clearly additional Cerenkov characteristics of spent fuel can be detected from off-alignment positions. In the case of the Atrium 9 x 9 fuel assembly, the three hidden water outlets under the lifting handle can be observed.

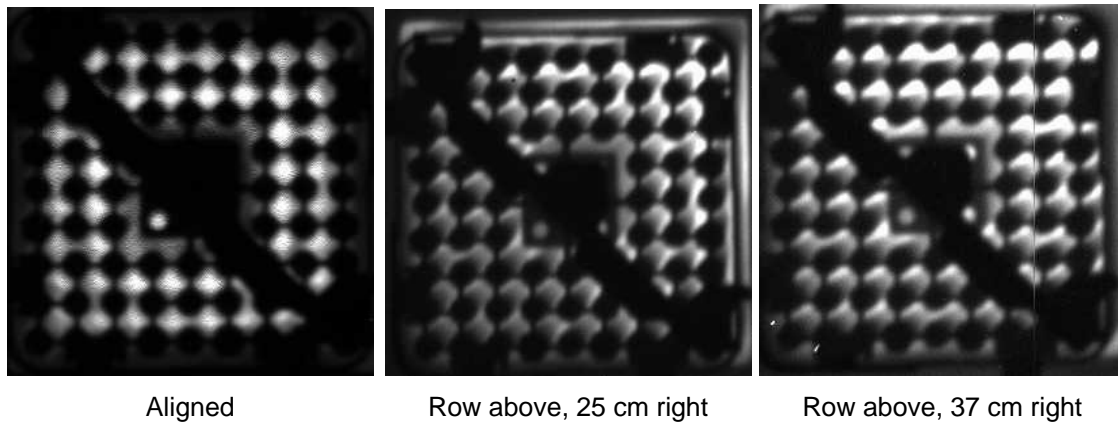


Figure 25: Cerenkov characteristics of an Atrium 9 x 9 fuel assembly from non-aligned positions

3.9 Quantitative Cerenkov characteristics—alignment

Alignment, the positioning of the DCVD directly above a fuel assembly such that maximum symmetrical intensity is observed in the image, is a key aspect of fuel verification with Cerenkov viewing devices. With the CVD, this characteristic is not quantifiable but it can be quantified with the DCVD.

Several images of fuel and non-fuels were taken at varying distances to the right of an assembly's aligned or 0 cm position. A number of these images are shown in Figure 26. The decrease in light intensity from the water spaces between the fuel rods is quite apparent for the spent-fuel assembly as the camera is moved to off-aligned positions. This

effect is less pronounced for the skeleton non-fuel assembly and still less for the high-density non-fuel.

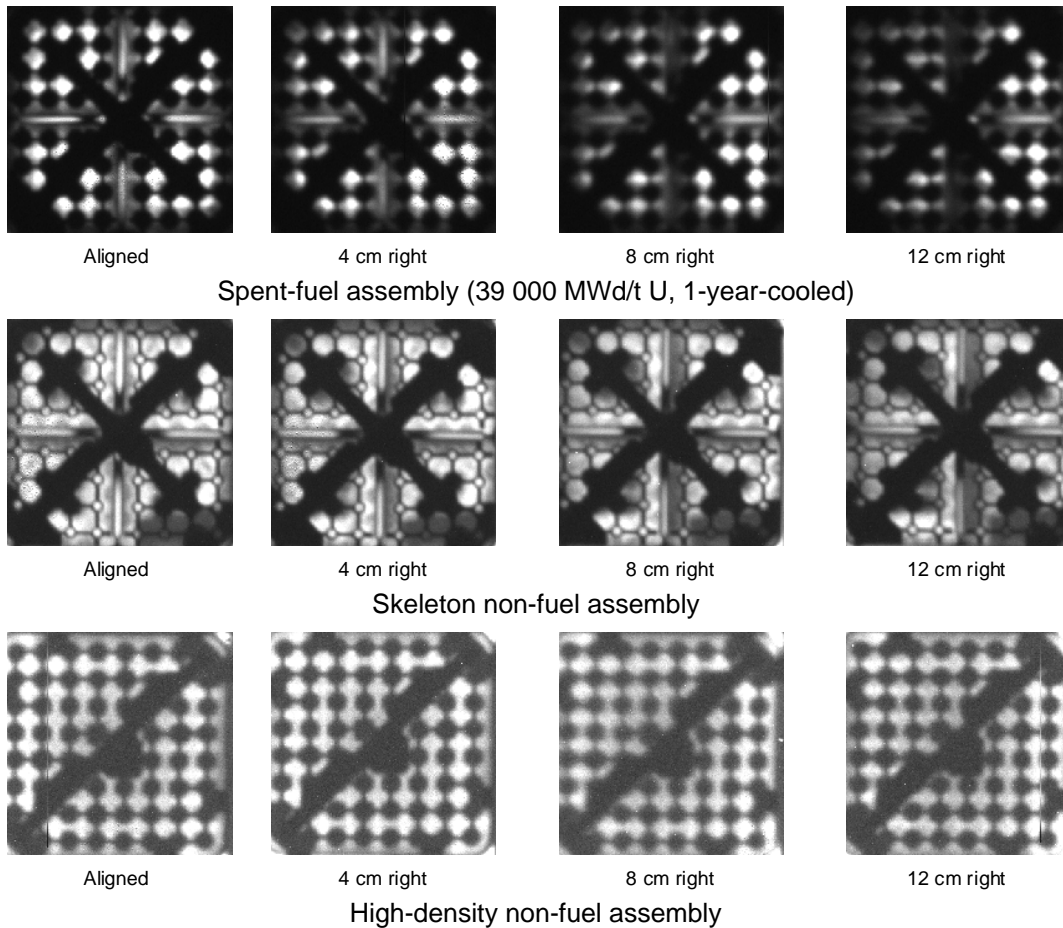


Figure 26: Alignment images for spent-fuel and non-fuel assemblies

To quantify this alignment effect, pixel intensities were obtained from each of the quadrants of the images (cf. the procedure described in Section 3.2). An example image (the 12 cm spent-fuel image) is shown in Figure 27. The pixels selected for averaging in each quadrant are indicated in red. The intensities obtained for the upper left quadrant for each of the assemblies is plotted in Figure 28. The high collimation of spent fuel is apparent in the slope of its curve while the non-fuel assemblies show substantially less collimation.

3.10 Cerenkov light fall-off from short-cooled spent fuel

Two applications for the measurement of the fall-off intensity in adjacent empty positions from spent-fuel assemblies are suggested here.

3.10.1 Correction for near-neighbour effects

The Cerenkov radiation from adjacent assemblies, i.e. the near-neighbour effect, can influence the intensity of Cerenkov light from spent-fuel assemblies, particularly long-cooled spent fuel. Knowing the fall-off characteristics of spent fuel, it may be possible to

calculate a background field for a specific assembly location based on its near neighbours. This background field could then be subtracted from the observed image, reducing or even eliminating the near-neighbour effect.

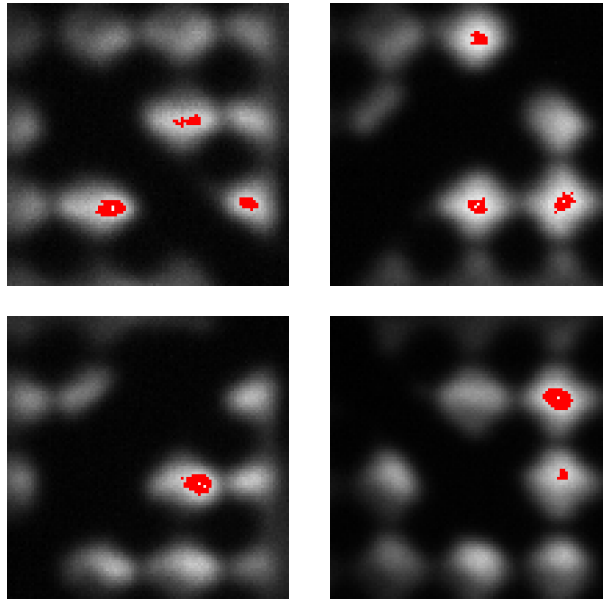


Figure 27: Selection of high intensity pixels in each quadrant

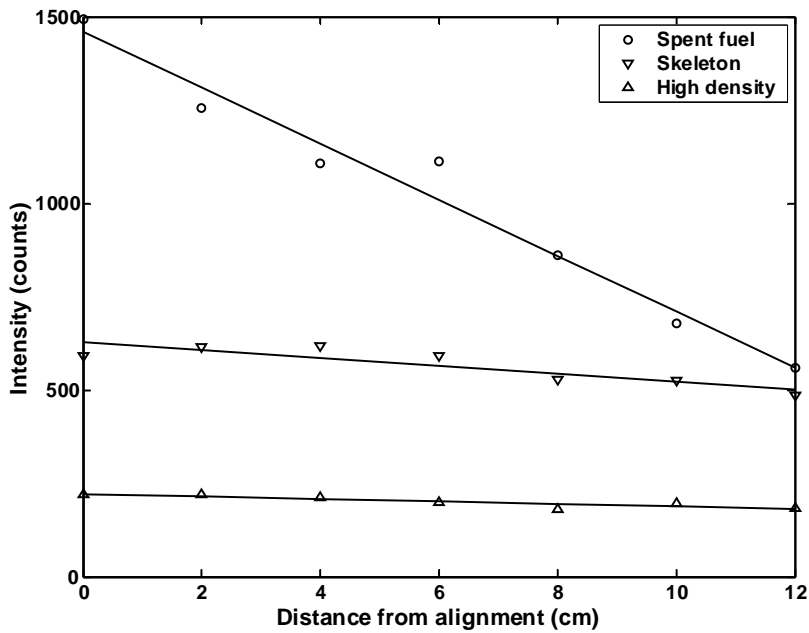


Figure 28: Alignment characteristic as a function of off-alignment distance

3.10.2 Verification of burnup and cooling time

Cerenkov light is generated in the water by the Compton process. The path length of the gamma ray and, therefore, the generation path length of Cerenkov light are proportional

to the energy of the gamma ray. Short-cooled fuel contains a relatively large number of radionuclides emitting high-energy gamma rays. These gamma rays should generate a broader Cerenkov glow than long-cooled fuel that contains relatively low-energy gamma emitters (primarily Cs-137). Knowledge of the fall-off characteristics may allow an independent verification of cooling time of spent fuel. The fall-off data obtained below provides only preliminary information for this development topic. Further field data is required and this topic will be left for a future report.

3.11 Quantitative near-neighbour corrections

Images obtained of a short-cooled spent fuel (39 000 MWd/t U, 1-year-cooled) and the empty fuel positions to its left are shown in Figure 29.

The intensity of the images was measured in two central water gaps in the spent-fuel assembly, then in the water gap just outside the spent-fuel position and in the centre of each of the four empty positions to the left. A plot of the image intensity versus the distance from the spent fuel is shown in Figure 30.

The rack pitch is 25 cm so the centre of each empty position is located at 25, 50, 75 and 100 cm to the left of the spent fuel. The intensities at these locations are shown on the graph as a percentage of the maximum value.

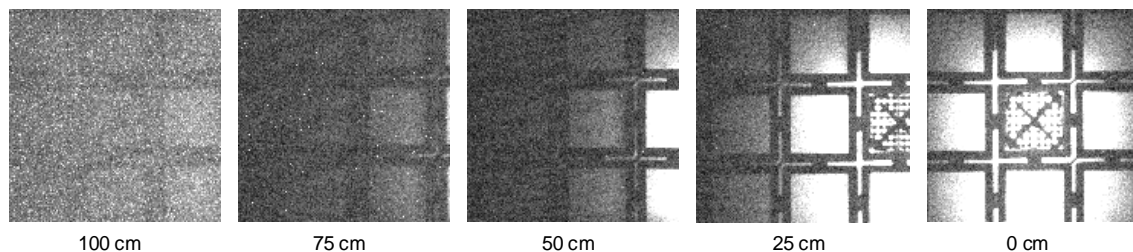


Figure 29: Fall-off of Cerenkov light from a spent-fuel assembly

The Cerenkov intensity in the centre of the first empty position is already down to 7% of the brightest location within the fuel. The rapid decrease in intensity beyond this first empty position suggests that any near-neighbour correction beyond one position would likely be negligible. These quantitative results are surprising because the first empty position appears very bright in both the DCVD and CVD. In fact, when looking at the Cerenkov DCVD or CVD image of the short cooled fuel assembly, one is not aware that the Cerenkov light emitted from between the fuel rods is about 15 times brighter than the light from a comparable area in an adjacent empty position.

The cross arrangement discussed in Section 3.3 provides a possible application for near-neighbour correction based on the curve in Figure 30. Although the fuels in the two arrangements differ in cooling times (1 year versus 4 years) the relative degree of near-neighbour correction should apply to the cross arrangement.

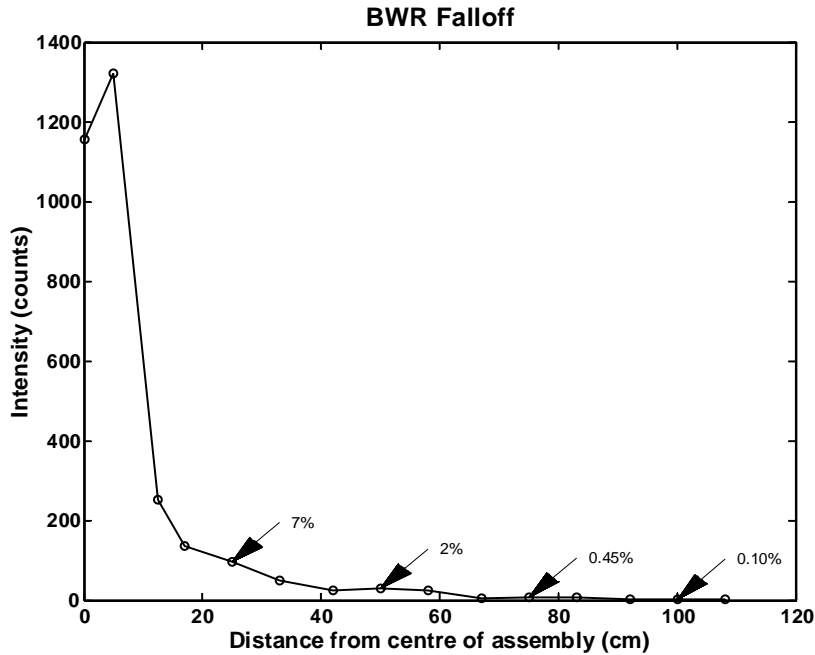


Figure 30: Intensity of Cerenkov light with distance from alignment

Assembly 18655 has one near neighbour; 18699 has two near and two corner neighbours; 18686 has four near and one corner neighbour. All assemblies in the cross arrangement are of nearly equal burnup and cooling time so we expect all their intensities to be fairly close. From Figure 30 we conclude that a near neighbour will contribute about 7% of its intensity while a corner neighbour, at 31 cm distant, would contribute about 4%. If the intensities of the fuels in the cross-arrangement fuels are roughly equal then the assembly with one near neighbour should be reduced by 7% ($3512/1.07 = 3282$). A similar procedure can be used for the other assemblies. The measured intensities and the corrected intensities are shown in Figure 31.

	3512 18655			3282 18655	
	3744 18699			3022 18699	
SF	4693 18686	SF	SF	3642 18686	SF
	SF	SF		SF	SF
Measured			Corrected		

Figure 31: Intensity values, measured and corrected for near-neighbour effects

If the assumptions on cross talk (Section 3.10) are correct, all of the corrected intensity values should be the same. Figure 31 shows that this is not true. In Section 3.10, the light

intensities of empty adjacent sites were measured. This is not identical to the situation in the above fuel arrangement where the near neighbour is contributing to the light intensity of an adjacent fuel assembly. The gamma radiation from the near neighbour is reduced by structures in the fuel assembly. This reduction does not occur in an empty site. This gamma ray absorption is mainly due to the fuel rods in the assembly.

More development work is obviously required to correct for near-neighbour effects. A long-term objective of this study is to obtain quantitative light intensities of spent fuel resulting in the possible estimation of cooling times and perhaps the burnup of spent-fuel assemblies.

4 FUTURE WORK

Previous studies using the DCVD instrument were centred on the determination of new information on Cerenkov characteristics of spent-fuel and non-fuel assemblies. The present study has turned more to the interpretation of the quantitative information available from the digital images. The software program Matlab was used to analyze the images for quantitative data. The present study has shown that additional information can be obtained from off angle images of fuel and non-fuel assemblies. More work is required in this area. Key to quantitative results is the need for precise data and more effort is required to obtain precision data. A number of fuel assemblies with missing and substituted rods were examined. DCVD images of these assemblies should be examined to determine if there is adequate statistical data to detect substituted fuel rods. More effort is required to understand the near-neighbour effect so that quantitative Cerenkov intensities can be obtained which can lead to determination of cooling time and perhaps burnup.

5 CONCLUSION

The DCVD instrument with the Marconi CCD47-20 back illuminated chip was successfully tested at Oskarshamn Unit 2 and Ringhals Unit 1 on BWR fuel and non-fuel assemblies. Excellent agreement was obtained between measured and theoretically calculated intensities of fuel assemblies with similar burnup but different cooling times. Characteristics of non-fuel assemblies have been identified that are different than spent-fuel assemblies. Fuel assemblies with missing fuel rods can be easily identified. More difficult is the detection of missing fuel rods that are hidden under fuel assembly structures such as the lifting handle. This needs further study and perhaps an off-angle view may solve this problem. The preliminary results from quantitative analysis of the Cerenkov images show great promise.

6 ACKNOWLEDGEMENTS

The authors would like to express their gratitude to the Oskarshamnsverkets Kraftgrupp, owner of the Oskarshamn nuclear power station, and The Ringhals Group, owner of the Ringhals nuclear power station, for making this study possible. We would like to thank their staff members for assistance in planning and conducting the tests.

The Swedish Support Program and the Canadian Safeguards Support Program funded these tests as part of their support programs for the International Atomic Energy Agency.

7 REFERENCES

- 1 J.D. Chen, L. Hildingsson, O. Trepte, E.M. Attas, G.R. Burton and G.J. Young; “Development of a high sensitivity Cerenkov viewing device: Concept SCCD field tests in Sweden”; CSSP Report 88, May 1996.
- 2 O. Trepte, L. Hildingsson, J.D. Chen, G.R. Burton, G.J. Young and E.M. Attas; “Development of a high sensitivity Cerenkov viewing device: Field test at Ringhals 2 PWR facility, Sweden”; SKI Report 94:45, October 1996.
- 3 J.D. Chen, E.M. Attas, G.R. Burton, G.J. Young, L. Hildingsson and O. Trepte; “Development of a high sensitivity Cerenkov viewing device: Concept SCCD CVD summary report”; CSSP Report 91, October 1996.
- 4 J.D. Chen, A.F. Gerwing, P.D. Lewis, M. Larsson, K. Jansson, B. Lindberg, E. Sundkvist, M. Ohlsson; “Development of a high sensitivity digital Cerenkov viewing device: Prototype digital Cerenkov viewing device field test in Sweden”; CSSP Report 123, SKI Report 01:8, May 2002.
- 5 J.D. Chen, A.F. Gerwing, R. Maxwell, M. Larsson, K. Axell, L. Hildingsson, B. Lindberg and E. Sundkvist; “Cerenkov characteristics of PWR assemblies using a DCVD with a back-illuminated CCD”; CSSP Report 2004-01-02, SKI Report ISRN SKI-R-03/46, November 2003.
- 6 S. Rolandson; “Determination of Cerenkov light intensities from irradiated BWR fuel”; SKI Report SE 1-94, January 1994.